https://doi.org/10.5194/egusphere-2023-477
Preprint. Discussion started: 21 March 2023

A numerical study on meltwater feedback in the coupled Arctic Sea ice-ocean system

Haohao Zhang[1], Xuezhi Bai[1], Kaiwen Wang[1]

[1]Key Laboratory of Marine Hazards Forecasting, Ministry of Natural Resources, Hohai University, Nanjing, 210098, China

Correspondence to: Xuezhi Bai (xuezhi.bai@hhu.edu.cn)

Abstract. A one-dimensional, coupled sea ice-ocean model is used to investigate the effects of meltwater on upper ocean stratification and sea ice melt and growth by decreasing the release of meltwater to the ocean. In the control experiments, the model is capable of accurately simulating seasonal changes in the upper ocean stratification structure compared to observations, and the results suggest that ocean stratification is important for ice thickness development during the growing season. The sensitivity experiments reveal the following: 1) A decrease in meltwater release weakens ocean stratification and creates a deeper, higher salinity mixed layer. 2) Meltwater release has negative feedback on ice melting, reducing ice melting by 19% by strengthening ocean stratification. 3) The impacts of meltwater release from the previous melting season on ice growth depend on the strength of stratification, with negative feedback (reducing ice growth by 14%) in areas with strong stratification and positive feedback (increasing ice growth more than 40%) in areas with weak stratification. 4) In some areas of the Nansen Basin where stratification is nearly absent, the warm Atlantic water can directly reach the ice in early spring, leading to early melting of the sea ice in winter if all meltwater is removed from the model. These findings contribute to our understanding of the complex interactions between ocean stratification, meltwater, and sea ice growth and have important implications for climate models and future change prediction in the Arctic.

1 Introduction

The upper Arctic Ocean is strongly stratified with primarily ice coverage and a high volume of freshwater input (Rawlins et al., 2010; Mcclelland et al., 2012; Rudels, 2015). The Arctic Ocean consists of three main layers. The top layer is a cold and fresh surface layer. The intermediate layer is a cold halocline layer (CHL), which is characterised by gradually increasing salinity, and the bottom layer is a relatively warm and salty Atlantic Water (AW) layer. This stratification pattern is crucial for the existence of Arctic Sea ice, as the fresh surface layer and CHL protect the ice cover from the heat stored in the AW layer below (Rudels et al., 1996; Steele and Boyd, 1998; Martinson and Steele, 2001; Rudels et al., 2005). Freshwater flux from river runoff, positive net precipitation, relatively fresh Pacific inflow, and seasonal ice melt are critical factors that maintain this stratification (Haine et al., 2015).

Ocean stratification plays a crucial role in determining the vertical heat flux, as well as in the growth and melting of sea ice. According to a one-dimensional coupled ice-ocean model study by Toole et al. (2010), the very strong density

https://doi.org/10.5194/egusphere-2023-477
Preprint. Discussion started: 21 March 2023

stratification at the base of the mixed layer in the Canada Basin greatly impedes surface layer deepening and thus limits the flux of deep ocean heat to the surface, which could influence sea ice growth and decay. Linders and Björk (2013) note that ocean stratification is mostly important for ice growth during the growing season because areas with weak stratification have larger ocean-to-ice heat fluxes, resulting in less ice formation during winter, but ice melting during the summer is basically independent of ocean stratification. Davis et al. (2016) use a one-dimensional model to show that the sea ice in the Eurasian Basin is more sensitive to changes in vertical mixing than that in the Canada Basin due to its weaker ocean stratification.

Seasonal ice melt is particularly important for seasonal changes in stratification in the Arctic Ocean (Jackson et al., 2010; Toole et al., 2010; Linders and Björk, 2013; Hordoir et al., 2022). During summer, approximately 11,300 km^3 of freshwater is produced by melting each summer and adds approximately 1.2 m of freshwater to the Arctic Ocean's surface (Haine et al., 2015). This creates a summer halocline that separates the surface mixed layer from the near-surface temperature maximum (NSTM), limiting vertical mixing and reducing heat flux from below (Jackson et al., 2010; Davis et al., 2016). In winter, surface fresh water is recycled via ice formation, weakening ocean stratification (Peralta-Ferriz and Woodgate, 2015).

It is reasonable to infer that meltwater can potentially create a feedback effect on sea ice melt and growth through its influence on seasonal changes in ocean stratification and oceanic heat flux. However, there are almost no quantitative studies on this kind of feedback, although many previous studies have investigated the effects of increased freshwater flux by adding freshwater flux to the ocean surface in models to represent an increase in runoff or precipitation (Nummelin et al., 2015; Davis et al., 2016; Nummelin et al., 2016; Pemberton and Nilsson, 2016).

To enhance the comprehension of meltwater feedback on sea ice, we use a one-dimensional coupled sea ice-ocean model and modify the source code to control the release of meltwater to the ocean to quantitatively assess the responses of ocean and sea ice to different amounts of meltwater release to the ocean. One-dimensional models have been widely used in previous studies of the Arctic Ocean's vertical structure and ice cover (Killworth and Smith, 1984; Price et al., 1986; Bitz et al., 1996; Björk, 2002a, 2002b; Peterson et al., 2002; Toole et al., 2010; Linders and Björk, 2013; Nummelin et al., 2015; Davis et al., 2016). A one-dimensional model is simplistic because it does not take into account advection processes; however, it usually provides a reasonable simulation of upper ocean stratification that matches observations well (Toole et al., 2010; Linders and Björk, 2013; Nummelin et al., 2015).

Additionally, the intensity of stratification varies across the Arctic Ocean, with a gradual weakening from the Canada Basin towards the Eurasia Basin. In the Canada Basin, a lower-saline upper layer results in a well-developed and persistent cold halocline (Toole et al., 2010). In contrast, the cold halocline layer is quite weak or even absent in some areas of the Eurasin Basin (Rudels et al., 1996; Steele and Boyd, 1998; Björk, 2002b), such as those close to Svalbard in the Nansen Basin, where the warm Atlantic waters are more easily mixed upwards and reach the ice cover (Rudels et al., 2005). Given the considerable spatial variability in the stratification strength across the Arctic Ocean, the impact of meltwater feedback is expected to vary regionally. The study investigates regional variations in the effect of meltwater on the ocean and sea ice by experimenting with the initial temperature and salinity profiles from multiple stations in the Arctic Ocean.

https://doi.org/10.5194/egusphere-2023-477
Preprint. Discussion started: 21 March 2023

The paper is organised as follows: Section 2 details the model setup and the sensitivity experiments. Section 3 presents the model results and discusses how the ocean and sea ice respond to reduced meltwater release. Section 4 reviews the conclusions, and a discussion is provided in sections 5.

2 Model description and sensitivity experiments

2.1 Coupled sea ice-ocean model

We use a one-dimensional, coupled sea ice-ocean model based on the Massachusetts Institute of Technology general circulation model (MITgcm) (Marshall et al., 1997) to explore the meltwater feedback in a coupled ice-ocean system in the Arctic Ocean. The water column in the model extends from the surface down to a depth of 300 m, and the vertical grid has a uniform thickness of 1 m. The ocean model utilises the nonlinear equation of state of Jackett and McDougall (1995) and the nonlocal K-Profile Parameterization (KPP) vertical mixing scheme of Large et al. (1994). The background vertical diffusivity is set to 10^{-6} m^2 s^{-1}, which is a representative value in the central Arctic Ocean (Fer, 2009).

The sea ice package is based on a variant of the viscous-plastic sea ice model (Losch et al., 2010) and is combined with the thermodynamic sea ice model of Winton (2000) and Bitz and Lipscomb (1999). The model considers two equally thick ice layers: the upper layer has a variable specific heat resulting from brine pockets, and the lower layer has a fixed heat capacity. The heat fluxes at the ice top and bottom are:

$$F_{top} = F_s(\alpha) - Fs_{ice} \quad (1)$$

$$F_{bot} = Fb_{ice} - F_b \quad (2)$$

where F_s is the surface heat flux absorbed by the ice, which is mainly influenced by the ice albedo α,

$$\alpha = \alpha_{i_{\min}} + \left(\alpha_{i_{\max}} - \alpha_{i_{\min}}\right)\left(1 - e^{-h_i/h_\alpha}\right) \quad (3)$$

where $\alpha_{i_{\min}}$=0.08 and $\alpha_{i_{\max}}$=0.64 are the maximum and minimum ice albedo values, respectively h_α=0.65 is the ice thickness for albedo transition, and h_i is the ice thickness.

F_b is the ocean-to-ice heat flux, $F_b = c_{sw}\rho_{sw}\gamma\left(T_{sst} - T_f\right)u^*$, γ is the heat transfer coefficient and u^* is the frictional velocity between ice and water. Fs_{ice} is the conductive heat flux from the upper layer of the sea ice to the ice surface, and Fb_{ice} is the conductive heat flux from the ice bottom to the lower layer of the sea ice, which are calculated by equations (4) and (5), respectively.

$$Fs_{ice} = \frac{4K_i(T_s - T_1)}{h_i} \quad (4)$$

$$Fb_{ice} = \frac{4K_i(T_2 - T_f)}{h_i} \quad (5)$$

where T_s is the skin surface temperature. K_i $(= 2.1656)$ is the constant thermal conductivity of sea ice. T_1 and T_2 are the temperatures of the upper and lower layers of sea ice, respectively.

The net ocean surface heat flux can be written simply as (Steele et al., 2010):

https://doi.org/10.5194/egusphere-2023-477
Preprint. Discussion started: 21 March 2023

$$F_{ocean} = F_{sw} + F_b + F_{ao} \quad (6)$$

where F_{sw} is the heat flux from solar radiation, F_b is the ocean to ice heat flux, and F_{ao} is the heat flux from the ocean to the atmosphere through the ice-free area (including longwave radiation and sensible and latent heat flux).

2.2 Initial conditions

The model is initialised with a given ice thickness (2.5 m), ice concentration (95%), and time-averaged temperature and salinity profiles measured by Ice-Tethered Profiles (ITPs) (Krishfield et al., 2008). The data from 11 ITPs are selected as initial profiles in the model simulations: A1-A5 located in the Amerasian Basin (the blue dots in Fig. 1) and E1-E5 in the Eurasian Basin (the yellow dots in Fig. 1), taken in April or May between 2011 and 2020. Data from other 6 ITPs are used to evaluate the simulation (the red dots in Fig. 1). The details of the ITP records are listed in Table 1.

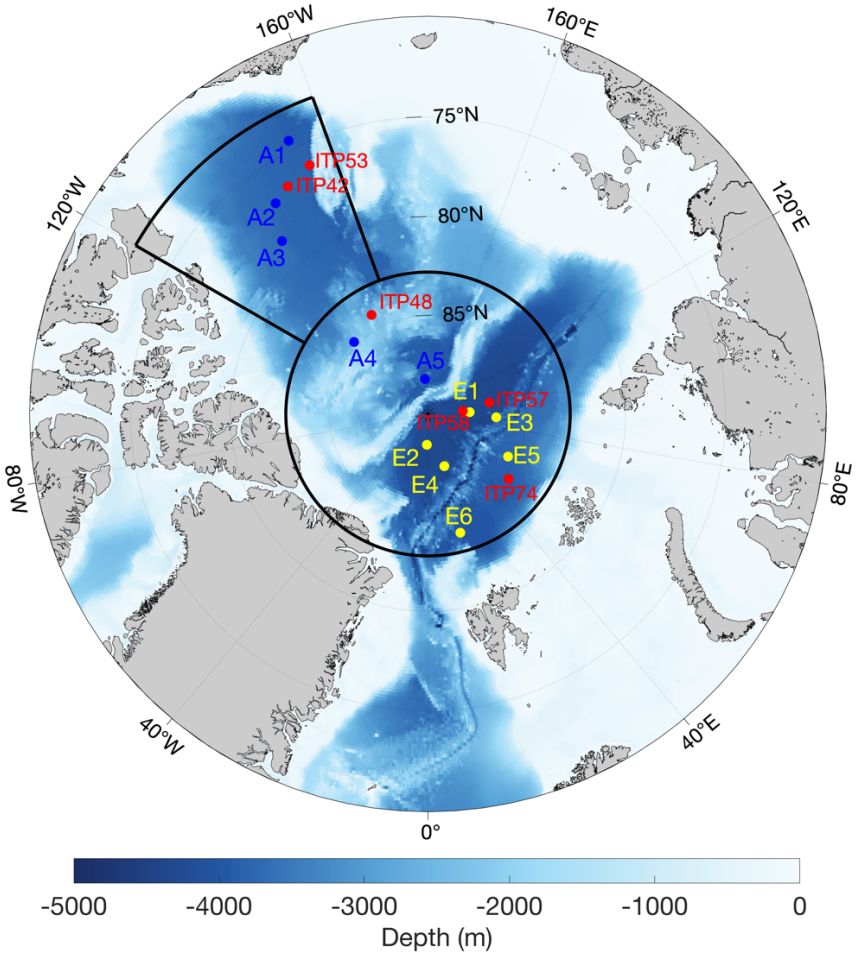

Figure 1: Positions of the ITP data used as initial profiles in the model simulations. Stations A1-5 are in the Americana Basin (the blue dots), and E1-E6 are in the Eurasian Basin (the yellow dots). The red dots denote the data used for comparison with the simulations. The bathymetry is from ETOPO-2, and the background colour indicates the ocean depth. The same atmospheric forcing field is used in all experiments and is derived from the 2011-2020 average for the specific region delineated by the solid black line.

https://doi.org/10.5194/egusphere-2023-477
Preprint. Discussion started: 21 March 2023

Table 1. Details of the ITP records used in in the model

Station	ITP number	Time	Comparison ITP number/Time
A1	ITP-53	2012.5.1-5.5	ITP-53/2012.8.1-8.5
A2	ITP-42	2011.4.1-4.15	ITP-42/2011.1.28-1.31
A3	ITP-41	2011.5.1-5.15	
A4	ITP-48	2012.5.9-5.23	ITP-48/2012.1.18-1.31
A5	ITP-47	2011.4.12-4.30	
E1	ITP-57	2013.5.25-5.28	ITP-58/2013.3.9-3.11
E2	ITP-56	2012.5.1-5.31	
E3	ITP-74	2014.5.26-5.31	ITP-57/2013.8.1-8.2
E4	ITP-58	2013.5.1-5.2	
E5	ITP-74	2014.5.26-5.30	ITP-74/2014.8.1-8.5
E6	ITP-111	2020.5.25-5.30	

Figure 2 shows the time-averaged vertical profiles of the temperature, salinity, and buoyancy frequency from the 11 ITPs. The buoyancy frequencies show that the strength of ocean stratification gradually decreases from the Pacific side towards the Atlantic side. The vertical profiles at stations A1, A2, and A3 display a warm water layer, a strong density gradient between 30 and 50 m and a temperature minimum at 175 m. The warm water layer and the strong density gradient are prominent throughout the central and western Canada Basin (Shimada et al., 2001; Steele, 2004) due to the intrusion of summer Pacific Water (sPW) and the freshwater input of the Mackenzie River, while the temperature minimum is due to the retention of winter Bering Sea water (Fig. 2a). Stations A4 and A5 are in the Makarov Basin, and the profiles show a transition feature from Pacific to Atlantic water influence. The upper layer of stations E1-E6 in the Eurasian Basin is characterised by a cold and fresh surface mixed layer overlying a deeper warm ($T > 0$°C) and salty Atlantic Water layer and weaker ocean stratification than the Amerasian Basin. These vertical profiles reflect various stratification features across the Arctic Ocean.

https://doi.org/10.5194/egusphere-2023-477
Preprint. Discussion started: 21 March 2023

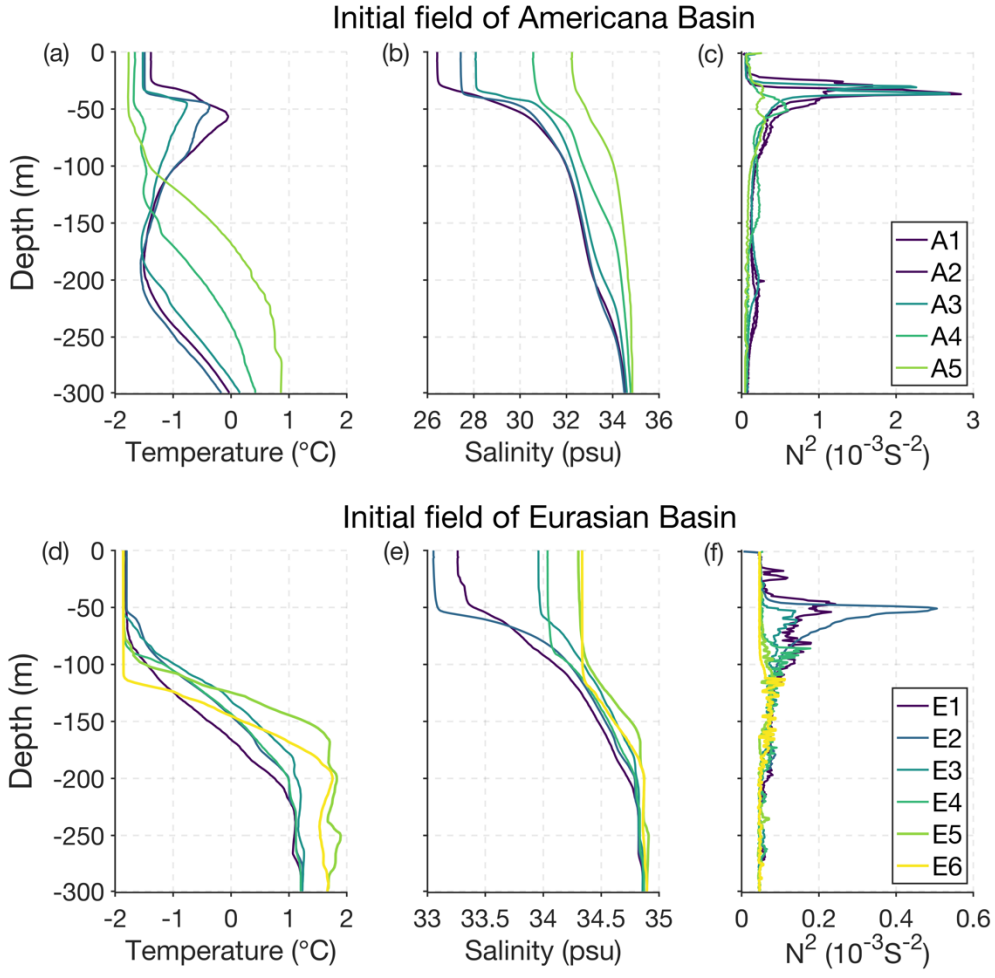

Figure 2: The observed temperature (a, d) and salinity (b, e) values obtained from ITP data between 2011 and 2020 in the Arctic Ocean, which are used as the initial profiles in the model simulations. The corresponding buoyancy frequency values (c, f) for each station are also displayed. The time of observation for each station is shown in Table 1.

2.3 Atmospheric forcing

Atmospheric forcing for the model includes daily 10-m wind speed, 2-m air temperature, 2-m specific humidity, and downwards long- and shortwave radiation, from the National Centers for Environmental Prediction-Department of Energy (NCEP-DOE) Reanalysis 2, all of which are regionally averaged over the area delineated by the black boundary in Fig. 1. The averages are calculated over the period of 2011 to 2020 and cover the area defined by the two subareas spanned by 83–90°N latitudes and 0–360°E longitudes (Central Arctic Ocean) and 73–83°N latitudes and 200–240°E longitudes (Canada Basin). Precipitation and runoff are not taken into account in these experiments. The same atmospheric forcing is used for all model runs to eliminate the effects of differences in atmospheric forcing.

https://doi.org/10.5194/egusphere-2023-477
Preprint. Discussion started: 21 March 2023

2.4 Sensitivity experiments

To explore how the release of meltwater affects ocean stratification and sea ice, six experiments are conducted at each station. The first is the control run, and the other five experiments are meltwater perturbation (MWP) runs with 0%, 20%, 40%, 60%, and 80% meltwater release into the ocean. In the coupled ice-ocean model, the meltwater flux of a timestep is determined by the freshwater content of the sea ice before and after a timestep. In its initial state, the freshwater content of the sea ice is as follows:

$$W_{frw} = \rho_{Ice} * H_{Ice} \quad (7)$$

where W_{frw} is the mass of fresh water initially present in the ice, ρ_{Ice} is the density of the ice (ρ_{Ice}= 900 kg m^{-3}) and H_{Ice} is the initial ice thickness. The meltwater entering the ocean is calculated as follows:

$$F_{reflx} = (W_{frw} - \rho_{Ice} * h_{Ice})/\Delta \quad (8)$$

where F_{reflx} (kg m^{-2} s)is the ocean freshwater flux and h_{Ice} is the ice thickness.

In the sensitivity experiments, we scale the freshwater flux by multiplying it by a factor k to control the amount of meltwater release:

$$F_{reflx} = k * \rho_{Ice} * (H_{Ice} - h_{Ice})/\Delta t \quad (9)$$

We set k to 0 (MWP-0% run), 0.2 (MWP-20% run), 0.4 (MWP-40% run), 0.6 (MWP-60% run), and 0.8 (MWP-80% run).

Figure 3a shows the time series of the ocean freshwater flux for the six experiments at station A1 as an example, in which the negative value represents freshwater entering the ocean. It is obvious that freshwater flux is negative (positive) during the ice-melting (ice-growth) season in the control runs. In the MWP runs, the freshwater flux is artificially reduced during the ice-melting season. As expected, the salinity gradient becomes weaker, and the mixed layer deepens when the release of the meltwater is reduced (Fig. 3b-g).

https://doi.org/10.5194/egusphere-2023-477
Preprint. Discussion started: 21 March 2023

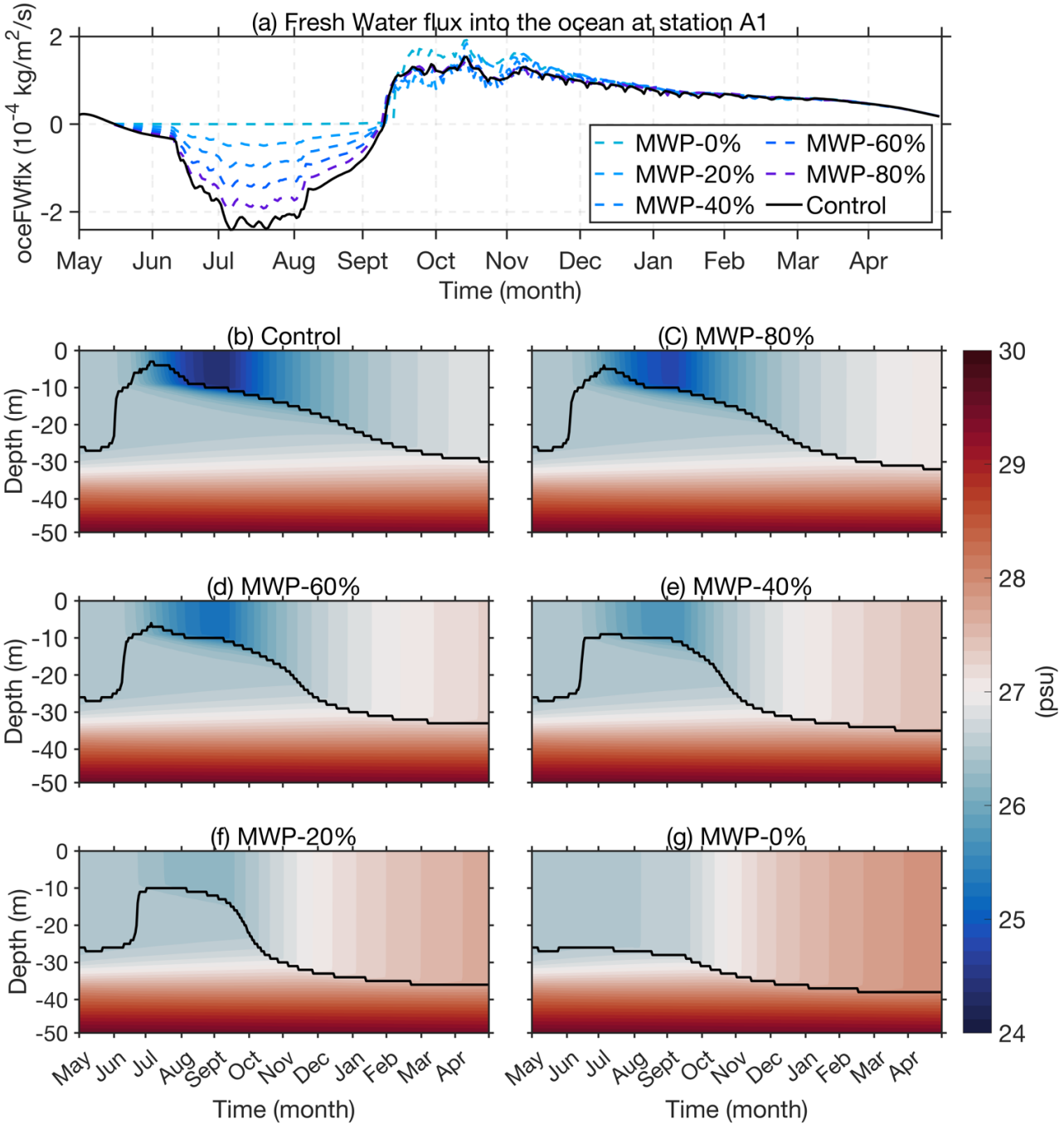

Figure 3: Simulated sea surface freshwater flux and time series of upper 50 m salinity at station A1. (a): Time series of sea surface freshwater flux. The negative values represent the freshwater entering the ocean. In the legend, ~% refers to the magnitude of the meltwater input anomaly in the MWP runs. (b): Time series of the upper 50 m salinity for the control run at station A1. (c)-(f): Time series of upper 50 m salinity for MWP runs at station A1. The black line in (b)-(g) indicates the depth of the mixed layer.

https://doi.org/10.5194/egusphere-2023-477
Preprint. Discussion started: 21 March 2023

3 Results

3.1 Control runs

3.1.1 Upper ocean thermohaline structure

Figure 4 shows the simulated temperature and salinity profiles at six stations in summer and winter in the control runs along with the ITP observations (details of the six ITP datasets are listed in Table 1 for comparison). We can see that the one-dimensional model results are reasonably consistent with the observations both in summer (Fig. 4a-c) and winter (Fig. 4d-f).

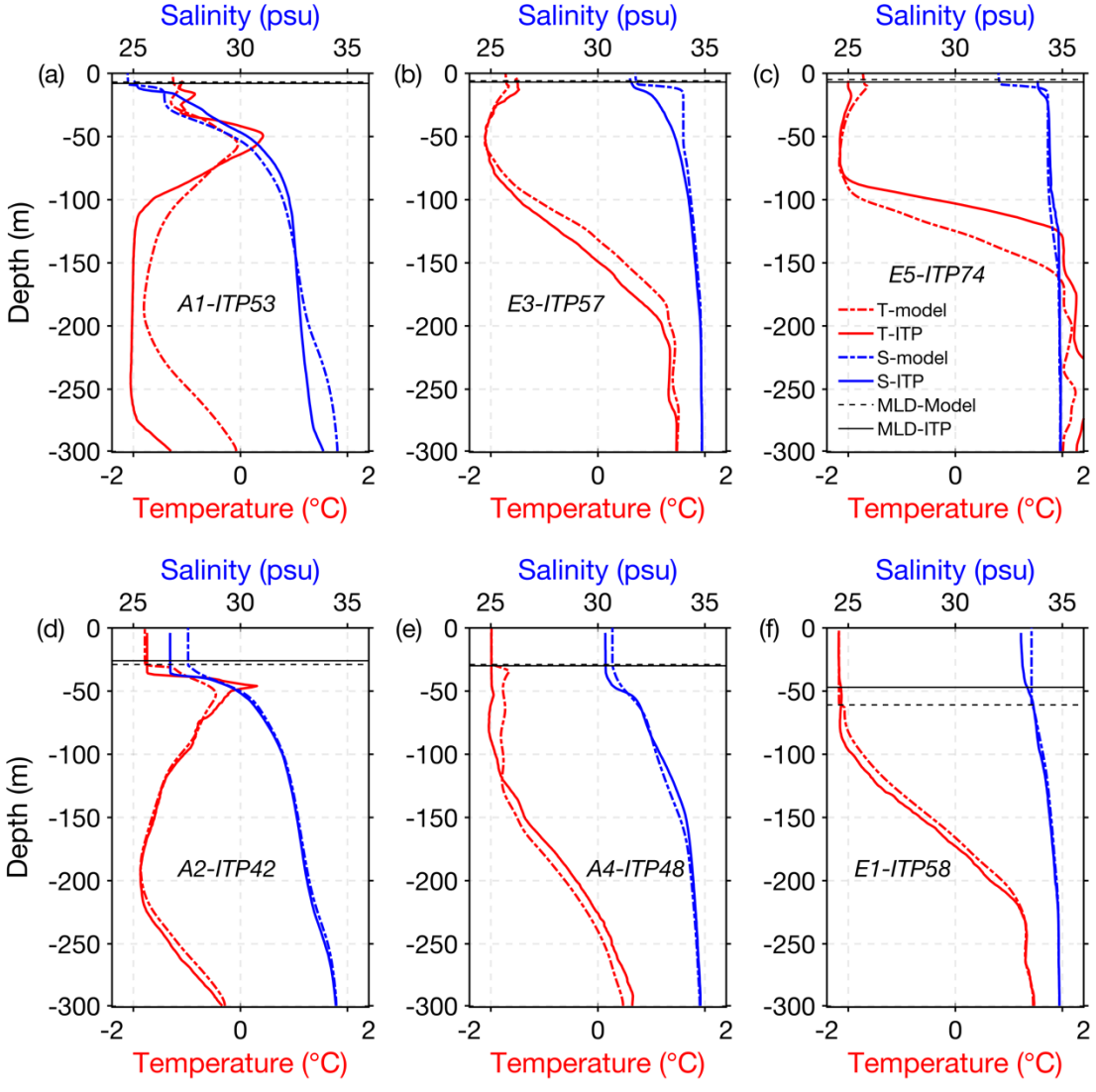

Figure 4: Comparison of the simulated temperature (red line) and salinity (blue line) (dotted line) with the nearby ITP data (solid line) during the melting (top row) and freezing seasons (bottom row). The depth of the mixed layer is indicated by the black lines parallel to the x-axis. (a): A1 and ITP-53 in August. (b): E3 and ITP-57 in August. (c): E5 and ITP-74 in August. (d): A2 and ITP-42 in January. (e): A4 and ITP-48 in January. (f): E1 and ITP-57 in April.

https://doi.org/10.5194/egusphere-2023-477
Preprint. Discussion started: 21 March 2023

During the melting season (May to September in the control runs), meltwater covers the ocean surface, creating a large salinity gradient between the surface and underlying water and forming a new, fresher surface layer. As shown in Fig. 4a-c, the simulated mixed layer depth (MLD) at stations A1, E3 and E5 in August is approximately 9 m, which is similar to that of nearby observations (note that the base of the ML is defined as the depth where the potential density relative to 0 dbar first exceeds the shallowest sampled density by 0.03 kg/m^3). The control runs successfully reproduce a warm water mass at the base of the mixed layer during summer (Fig. 4a-c), which Shimada et al. (2001) refer to as "Summer Mixed Layer Water" and Jackson et al. (2010) refer to as the Near-Surface Temperature Maximum (NSTM). The NSTM is a local, seasonal feature caused by penetrative shortwave solar heating, principally through leads, which is closely associated with sea ice melting/formation (Perovich and Maykut, 1990; Shimada et al., 2001; Jackson et al., 2010).

During the freezing season (October to the following April in the control runs), brine rejection enhances the turbulence scale perturbations, leading to a deeper mixed layer, and the NSTM progressively cools and vanishes (Fig. 4d-f). Both the modelling and the observations show that the mixed layer is deeper in the western Arctic than in the eastern Arctic. In all control runs, the simulated maximum winter MLD ranges from 30 to 34 m in the Canadian Basin, 44–61 m in the Makarov Basin, 59–103 m in the Amundsen Basin, and 119–136 m in the Nansen Basin. These results are comparable to the observations. The observed maximum winter MLDs in Canada and the Makarov Basin are 29 ± 12 m and 52 ± 14 m, respectively, and those in the Eurasian Basin range from ~50 to over 100 m, with large regional differences (Sirevaag et al., 2011; Peralta-Ferriz and Woodgate, 2015).

3.1.2 Sea ice and ocean ice heat flux

Figure 5 shows the temporal development of ice thickness, ice concentration and ocean-ice heat flux in the control runs. The amount of ice melt during the melting season ranges from 1.33 m to 1.39 m across all stations, which is basically independent of the initial ocean stratification. However, the sea ice growth shows dependence on the initial ocean stratification (Fig. 5a). Under the same atmospheric forcing, stations in the Canada Basin (A1-A5) with well-developed and persistent haloclines have more ice growth (1.76-1.79 m), while stations E5 and E6 in the Nansen Basin have less ice growth (1.61 m and 1.59 m, respectively) because the cold halocline is not fully developed there, and consequently, the higher ocean ice heat flux from February to April inhibits ice formation (Fig. 5c).

https://doi.org/10.5194/egusphere-2023-477
Preprint. Discussion started: 21 March 2023

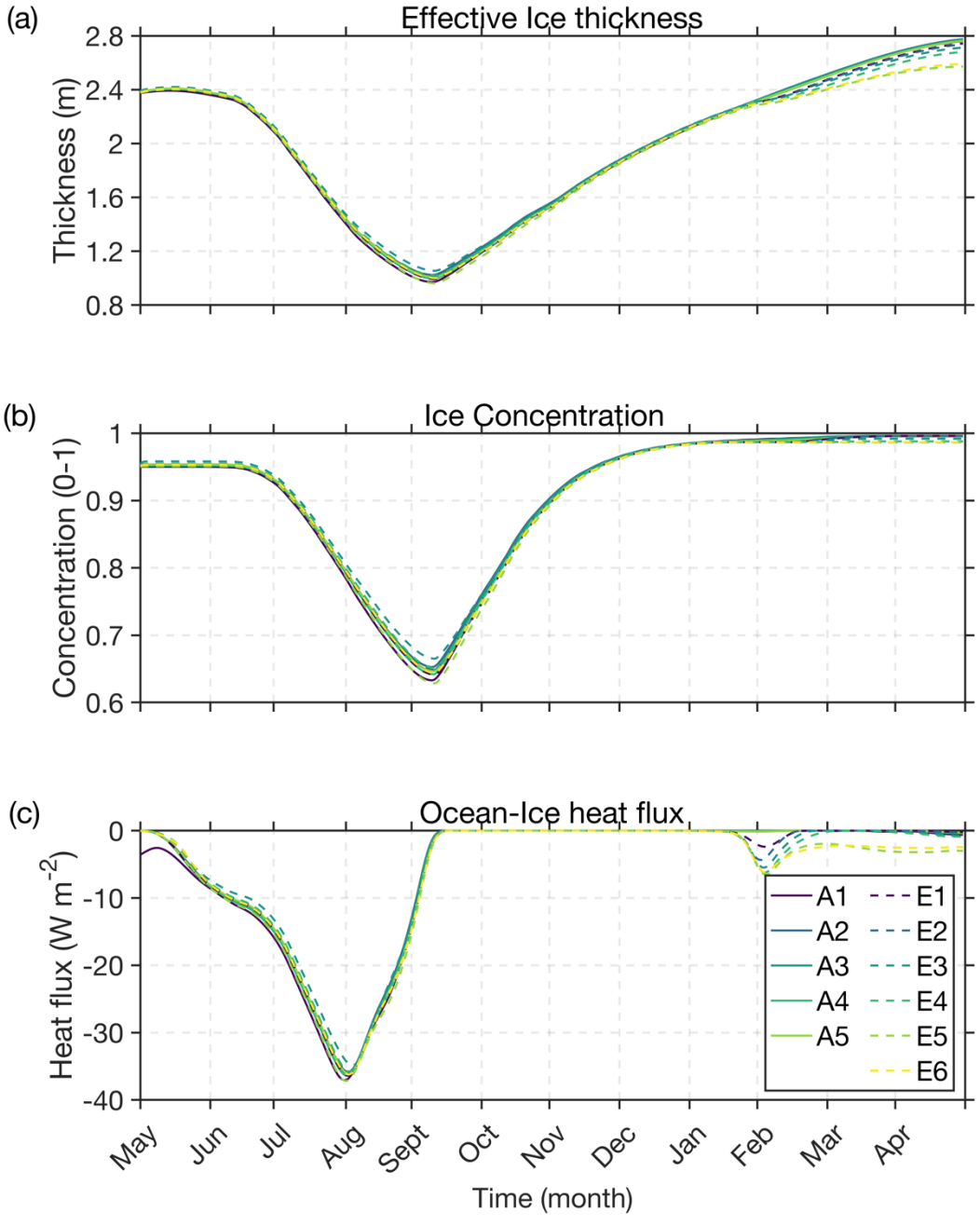

Figure 5: The control run results of the (a) effective sea ice thickness, (b) ice concentration and (c) ocean to ice heat flux (negative values represent the loss of heat from the ocean) for all control runs.

https://doi.org/10.5194/egusphere-2023-477
Preprint. Discussion started: 21 March 2023

In the control run, the calculated ocean-ice heat flux in the Canada Basin (stations A1-A5) has an average value of 0.04 W/m2 during the freezing season and 15.9 W/m2 during the melting season (Fig. 5c). The observed ocean ice heat flux from the entire surface heat budget of the Arctic Ocean (SHEBA) drift has an average value of 2.2 W/m2 during winter and 16.3 W/m2 during summer (Shaw et al., 2009). This comparison indicates that the simulated ocean-ice heat flux is close to the observations in summer but much smaller than the observations in winter. The main reason for this is the omission of horizontal advection in the one-dimensional model. The horizontal heat advection is an important heat source during winter, and omitting it from the model will lead to a lower ocean ice heat flux. However, in summer, the main heat source is the absorption of solar radiation (Linders and Björk, 2013) and the surface water temperature is less affected by horizontal heat advection.

Simulated ocean-ice heat fluxes in the Amundsen Basin (station E1-4) and Nansen Basin (station E5-6) have an average value of 0.37 W/m2 and 1.3 W/m2 during the freezing season and 15.47 W/m2 and 16.1 W/m2 during the melting season (Fig. 5c), respectively. The ocean ice heat flux in the Eurasian Basin in winter is larger than that in the American Basin, which results in less ice formation in the Eurasian Basin. The results suggest that ocean stratification is a very important factor for ice growth, which agrees with the conclusions of Linders and Björk, (2013).

3.2 Melt water perturbation experiments

3.2.1 Upper ocean responses

a) Summertime

Figure 6 shows the temperature and salinity profiles in summer for the MWP and control runs. It is obvious that no release of meltwater has the most pronounced effects, compared to the control run, while the release a portion of meltwater has moderate to little effect on the upper ocean thermostructure.

In the MWP-0% runs, as no meltwater is released, the upper water is well mixed, the NSTM vanishes, and the temperature and salinity are uniform in the upper layer (down to a depth of several tens of meters) in the Canada Basin to more than a 100 metres depth in the Nansen Basin. As a result of mixing, compared with the control run, salinity increases and temperature decreases in the mixed layer at stations A1-A5 and E1-E3. However, at stations E4, E5 and E6, the temperature decreases in the upper mixed layer but increases in the lower layer (Fig. 6c-e). Those stations have weak stratification, and the removal of all meltwater enhances mixing, which transfers heat stored in the NSTM downwards, thereby warming the lower mixed layer.

https://doi.org/10.5194/egusphere-2023-477
Preprint. Discussion started: 21 March 2023

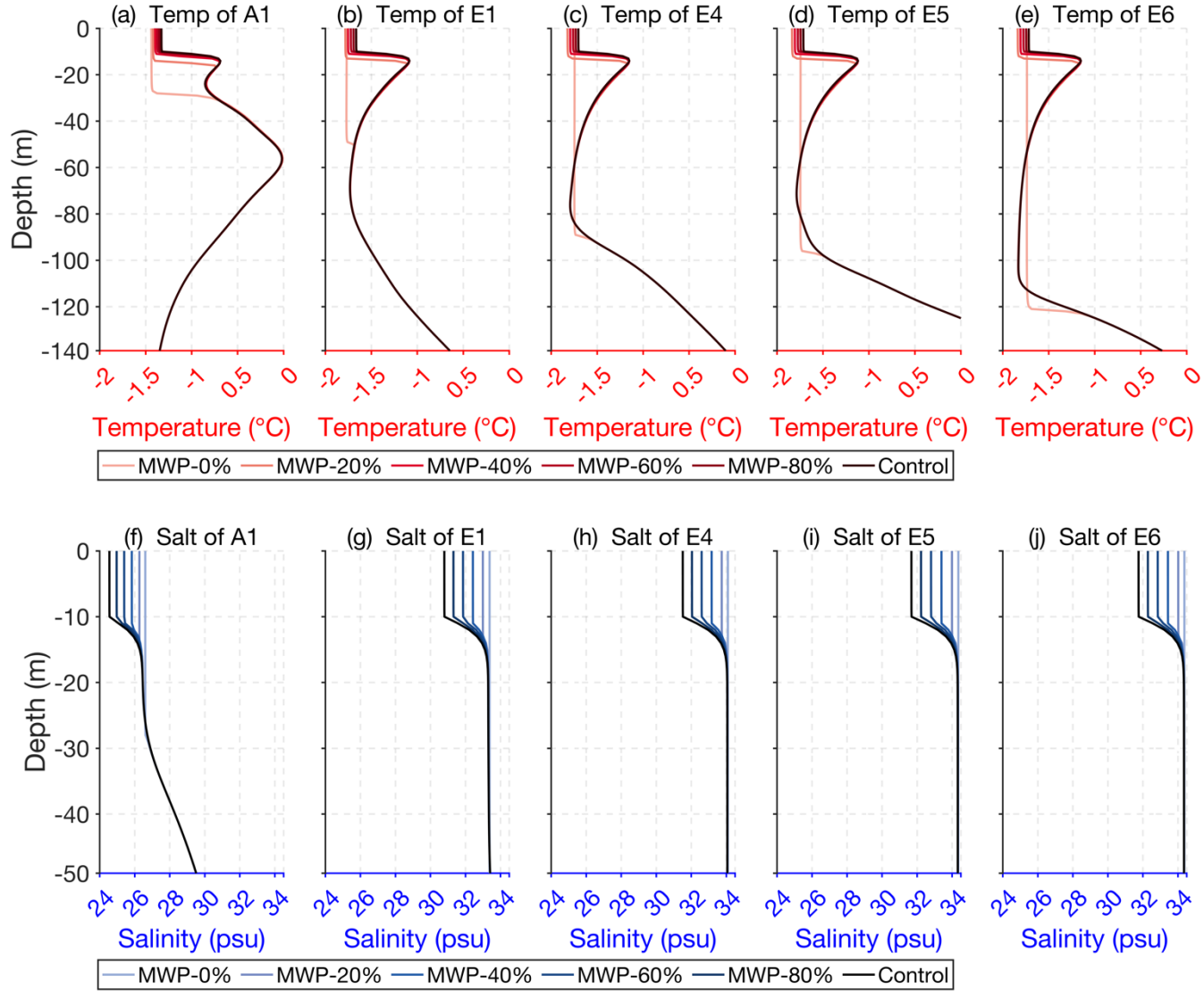

Figure 6: Simulated temperature (top row) and salinity (bottom row) profiles of MWP runs and control runs in mid-August for stations A1, E1, E4, E5 and E6.

In contrast to the MWP-0% run, the summer MLD in the MWP 20%-80% runs are no more than 10m, which implies that a certain amount of meltwater is sufficient to maintain upper ocean stratification during summer. When all the meltwater is removed from the model, the MLD can reach 28 m at station A1, 50 m at station E1, 90 m at station E4, 108 m at station E5 and 122 m at station E6 at the end of the melting season (Fig. 7).

https://doi.org/10.5194/egusphere-2023-477
Preprint. Discussion started: 21 March 2023

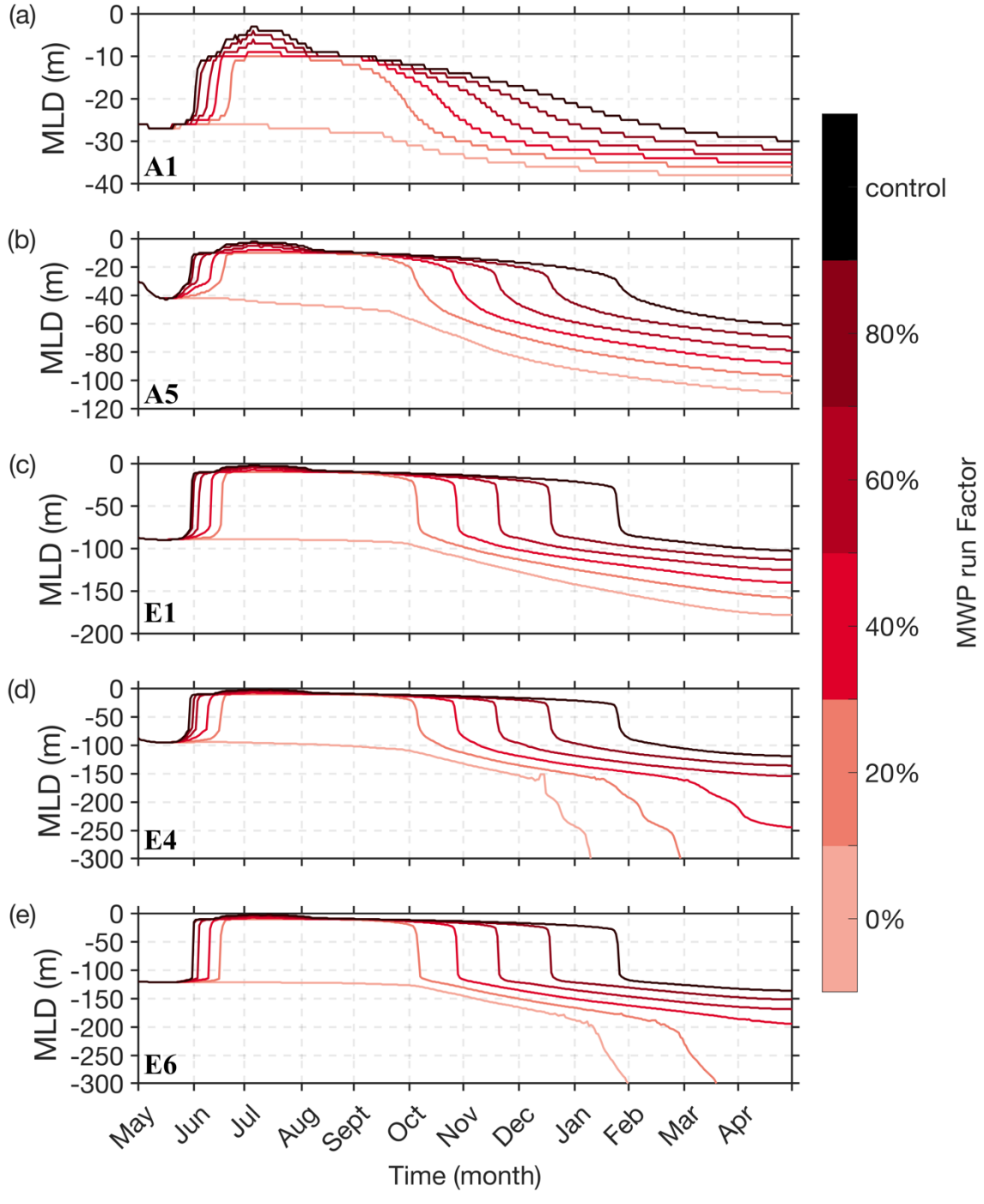

Figure 7: Time series of the MLD of the control and MWP runs for stations (a) A1, (b) A5, (c) E1, (d) E4, and (e) E6. The colour of each line represents the MWP run factor.

https://doi.org/10.5194/egusphere-2023-477
Preprint. Discussion started: 21 March 2023

b) Wintertime

Figure 8 shows the temperature and salinity profiles in winter for the MWP and control runs. The extent to which meltwater affects the ocean profile varies with stations (Fig. 8). At each station, the MLD increases following the reduction in the release of meltwater in the previous melting season. Close to the end of the freezing season (mid-April), the MLD reaches its maximum at all stations. At stations A1-A3 in the Canada Basin, the MLD is 38 m for the MWP-0% run and is still unable to penetrate the warm Pacific water layer (Fig. 7a). The MLD in the Amundsen Basin is much larger than that in the Canada Basin in the MWP-0% runs; for example, the MLD is 107 m (62 m in the control run) at station E1 and 169 m (103 m in the control run) at station E4 (Fig. 7b-d). Nevertheless, it is still unable to reach the core of the warm Atlantic water.

Stations E5 and E6 in the Nansen Basin show a relatively extreme situation in the 0% and 20% runs during winter. The removal of all the meltwater leads to the mixed layer dropping to a depth of more than 300 m (135 m and 120 m in the control run, respectively), which can reach the core depth of the warm Atlantic waters (Figs. 7d and e). This led to a dramatic change in the structure of the vertical profile when the Atlantic water layer was well mixed with the cold water in the upper layers (Fig. 8d, e, i and j). The heat carried by the warm Atlantic waters will melt the surface ice and release significant amounts of heat into the atmosphere, as described in the next section. The results suggest that the positive buoyancy flux of the meltwater is a significant impediment to the deepening of the mixed layer throughout the simulation.

The above results of the MWP runs imply that the subsurface warm Pacific water in the Canada Basin is unable to reach the ice even when all the meltwater is removed due to strong stratification. However, at some places in the Nansen Basin, such as at stations E5 and E6, that lack a fully developed halocline, meltwater plays an important role in preventing the mixed layer from reaching the Atlantic water layer.

https://doi.org/10.5194/egusphere-2023-477
Preprint. Discussion started: 21 March 2023

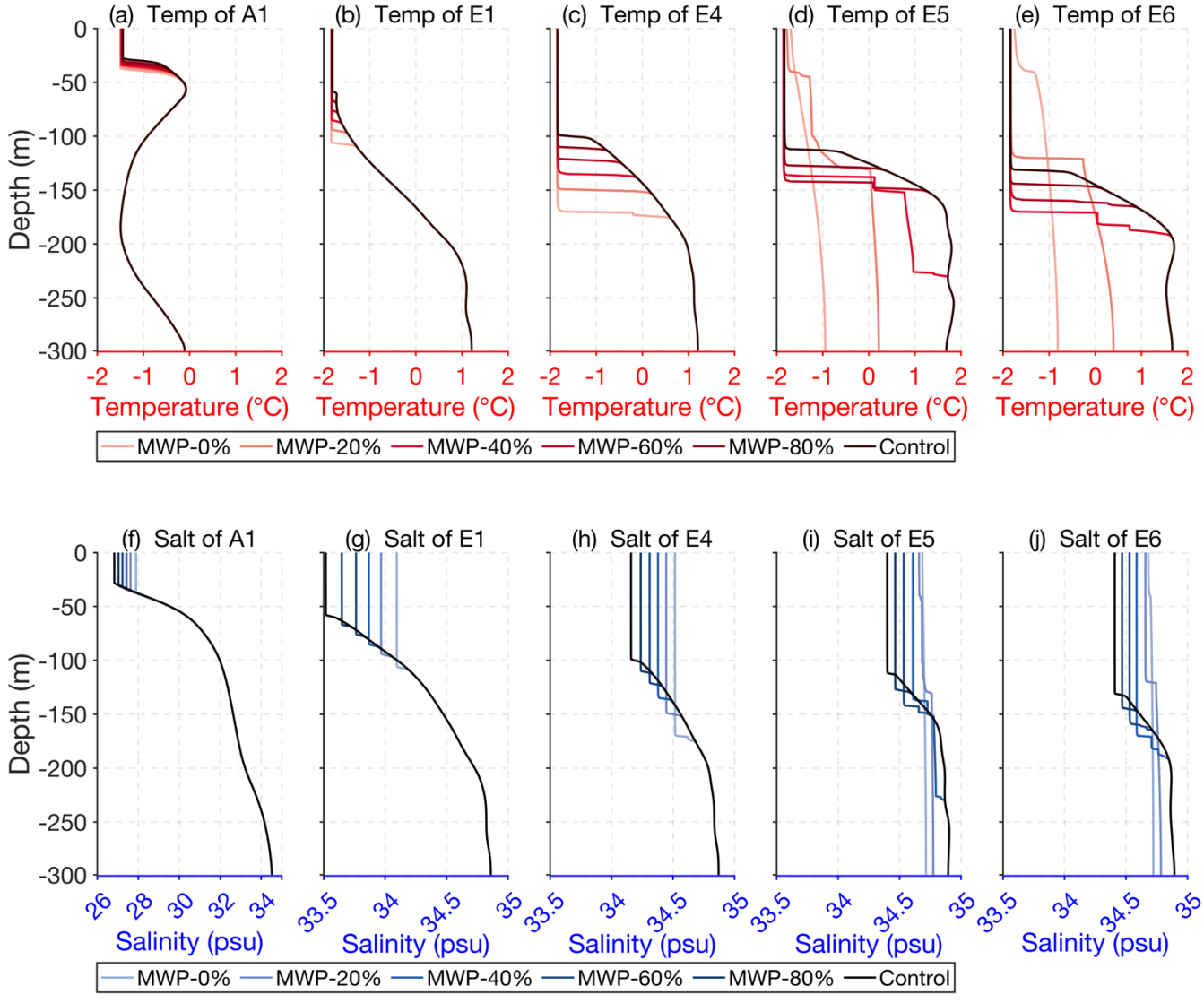

Figure 8: Same as Fig. 6 but in mid-April.

3.2.2 Sea ice responses

a) Melting season

The reduced meltwater release leads to decreases in the summertime effective ice thickness and ice concentration (Fig. 9). The ice melting season is also significantly prolonged when all the meltwater is removed (Fig. 9). In comparison to the control run, the amount of melting ice increases by 19.6 cm (~14.4%), 6.5 cm (~4.8%), 3.8 cm (~2.8%), 2.3 cm (~1.8%) and 1.2 cm (~0.9%) (averages of all stations) for the MWP-0%, 20%, 40%, 60% and 80% runs, respectively, over the entire melting season (Fig. 10a). This suggests that the removal of meltwater promotes ice melting, i.e., meltwater has negative feedback on sea ice melting

https://doi.org/10.5194/egusphere-2023-477
Preprint. Discussion started: 21 March 2023

during summer. Moreover, the extent of the meltwater effect on ice melting varies between stations. The feedback effect on sea ice melting is more significant at stations with strong stratification. For instance, in the MWP-0% run, the rate of summer ice melting increases by over 18% at stations located in the Canadian Basin. In contrast, there is only a slight increase of 7% at station E6 in the Nansen Basin (Fig. 11a).

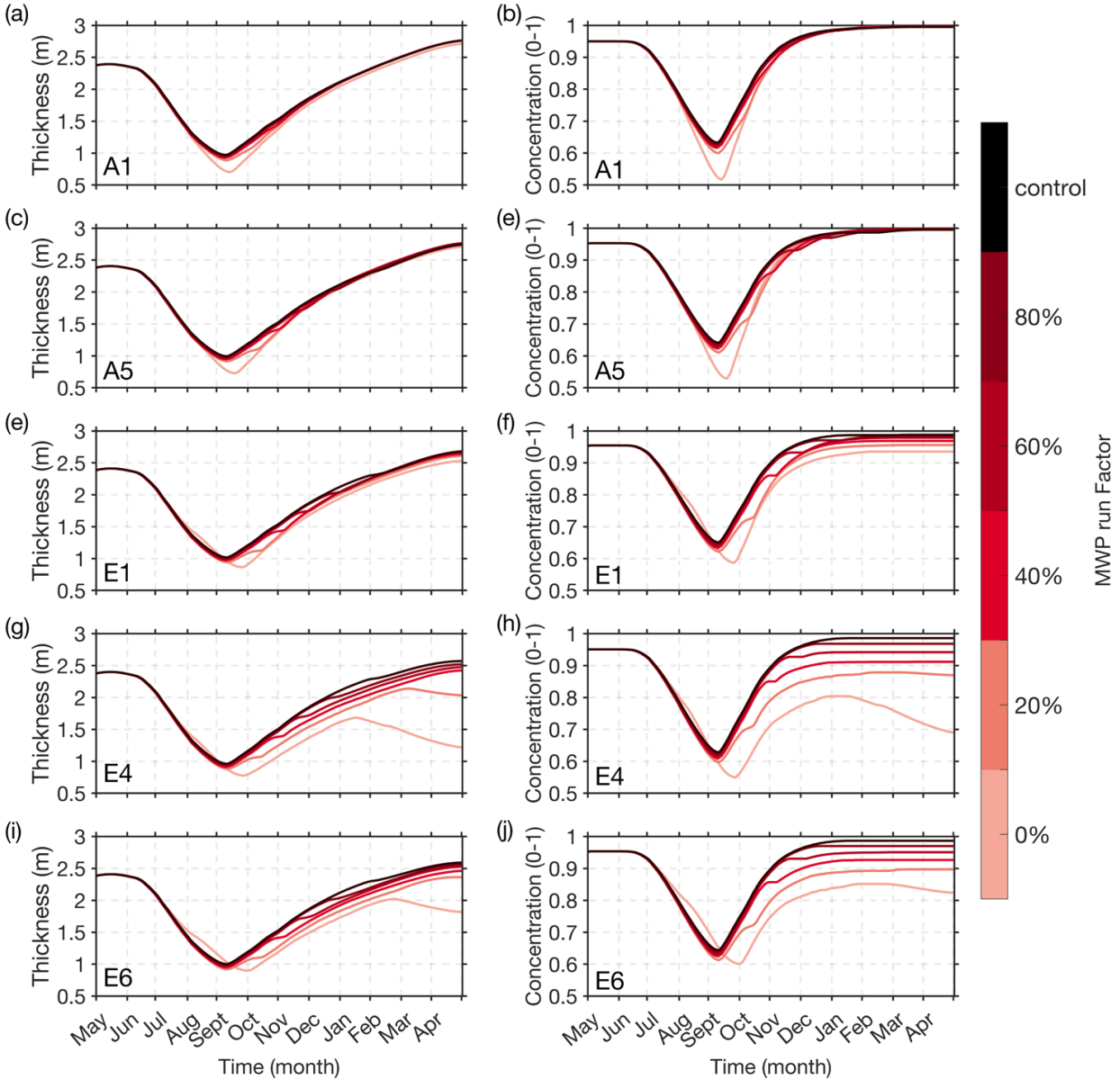

Figure 9: Same as Fig. 7 but for the (left) effective ice thickness and (right) ice concentration.

https://doi.org/10.5194/egusphere-2023-477
Preprint. Discussion started: 21 March 2023

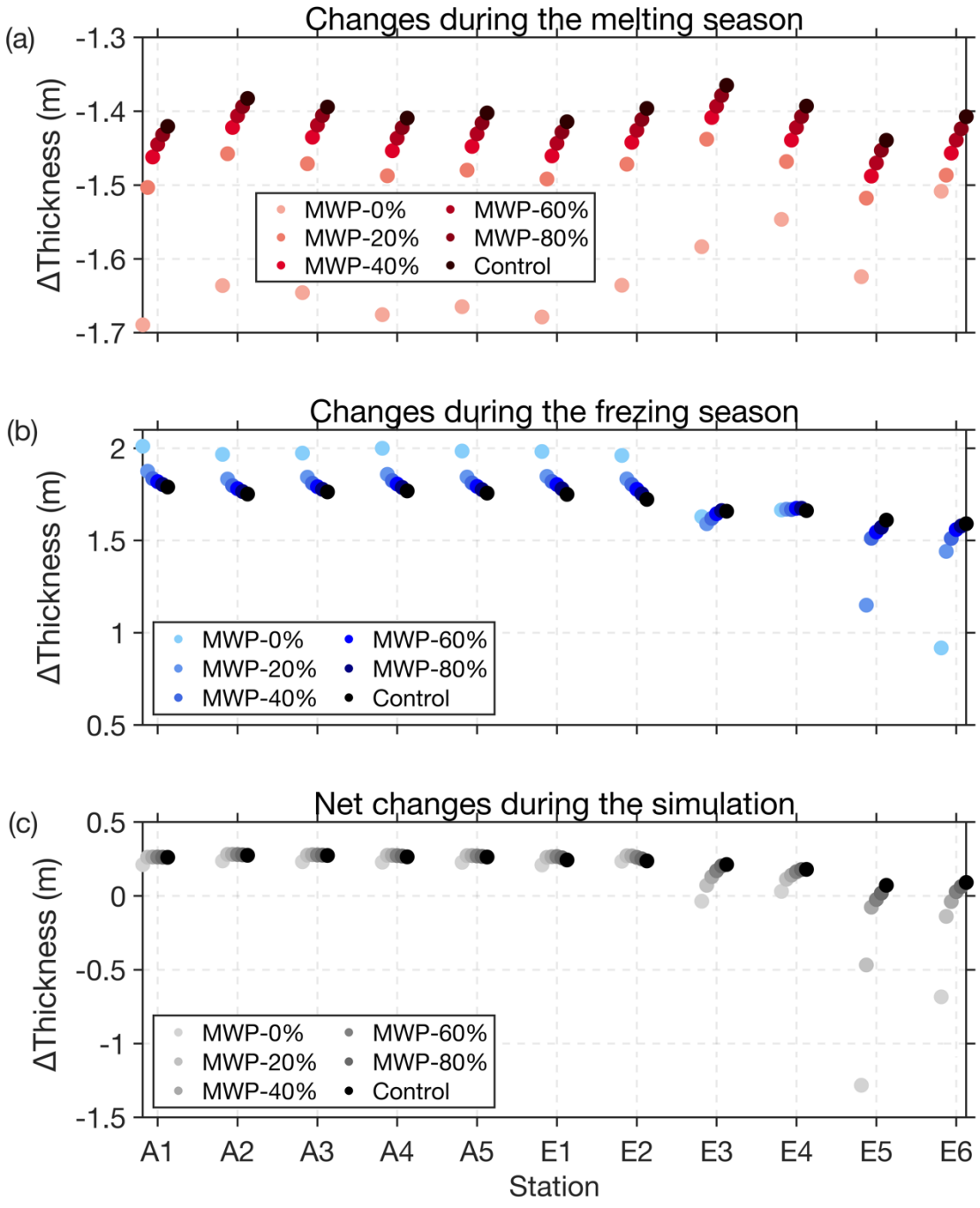

Figure 10: Ice thickness change during model simulation for all stations. (a) Effective ice thickness change during the melting season. (b) Effective ice thickness change during the freezing season. (c) Difference in effective ice thickness between the end value and the initial value.

https://doi.org/10.5194/egusphere-2023-477
Preprint. Discussion started: 21 March 2023

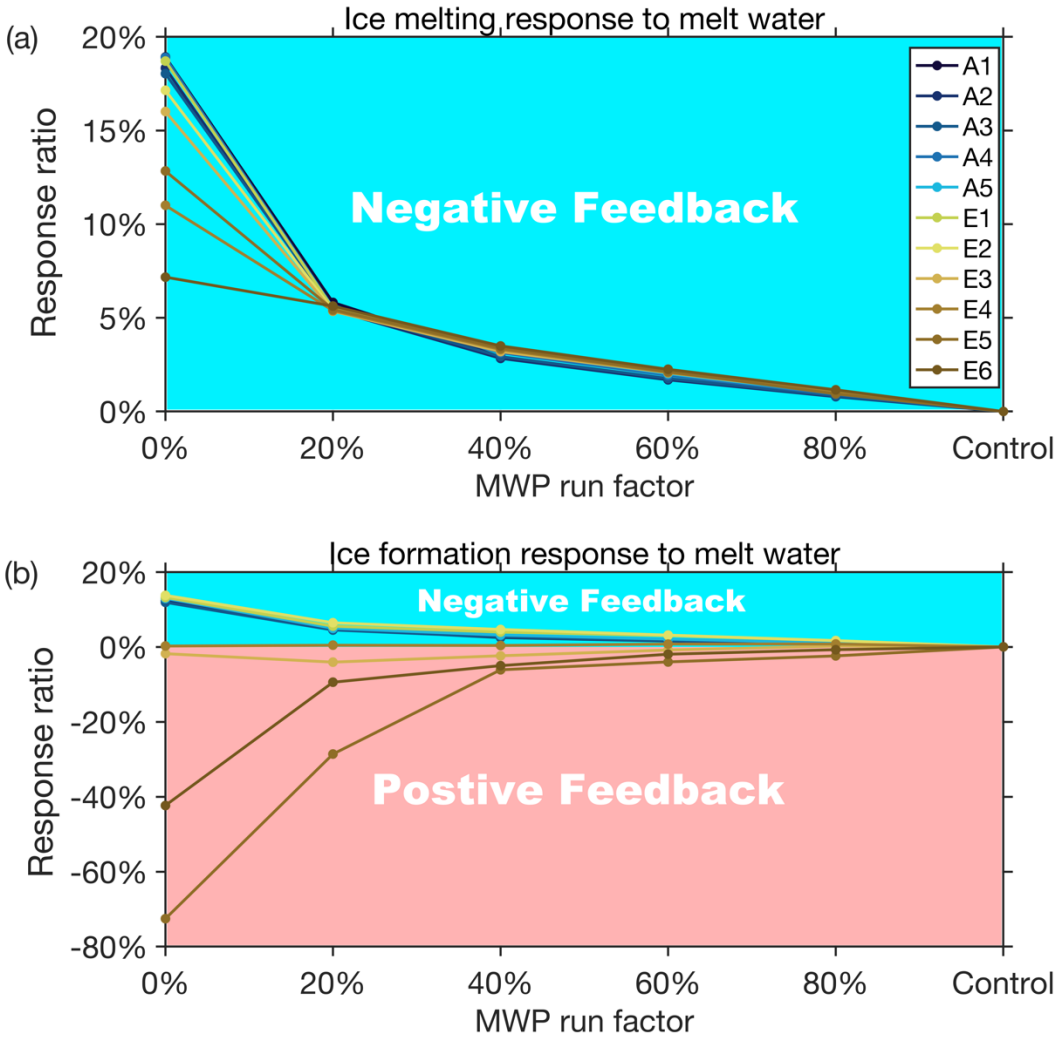

Figure 11: Simulated (a) summer and (b) winter percentage change in sea ice relative to the control run in response to decreasing meltwater. (a): After reducing the release of meltwater, the amount of ice melting increased at all stations, indicating that the release of meltwater hindered ice melting; that is, meltwater had a negative feedback effect on ice melting. (b): After reducing the release of meltwater, the amount of ice formation increased at stations A1-5 and E1-2, indicating that the release of meltwater hindered ice formation at these stations; that is, meltwater had a negative feedback effect on ice formation at these stations. In contrast, the amount of ice formation at stations E5 and E6 significantly decreased after reducing the release of meltwater, indicating that the release of meltwater can promote ice formation at these stations; that is, meltwater has a positive feedback effect on ice formation at these stations.

The time series of the ice top and bottom melting rate differences between the MWP and the control runs are shown in Fig. 12. The meltwater feedback acts mainly on the ice bottom, as opposed to on the ice top. The meltwater affects bottom melting mainly by impeding vertical mixing of the heat stored in the NSTM. In the MWP-20% to -80% runs, as the meltwater release decreases, the summer halocline weakens, allowing more heat in the NSTM to mix upwards, resulting in a larger ocean ice heat flux (Fig. 13, left column).

https://doi.org/10.5194/egusphere-2023-477
Preprint. Discussion started: 21 March 2023

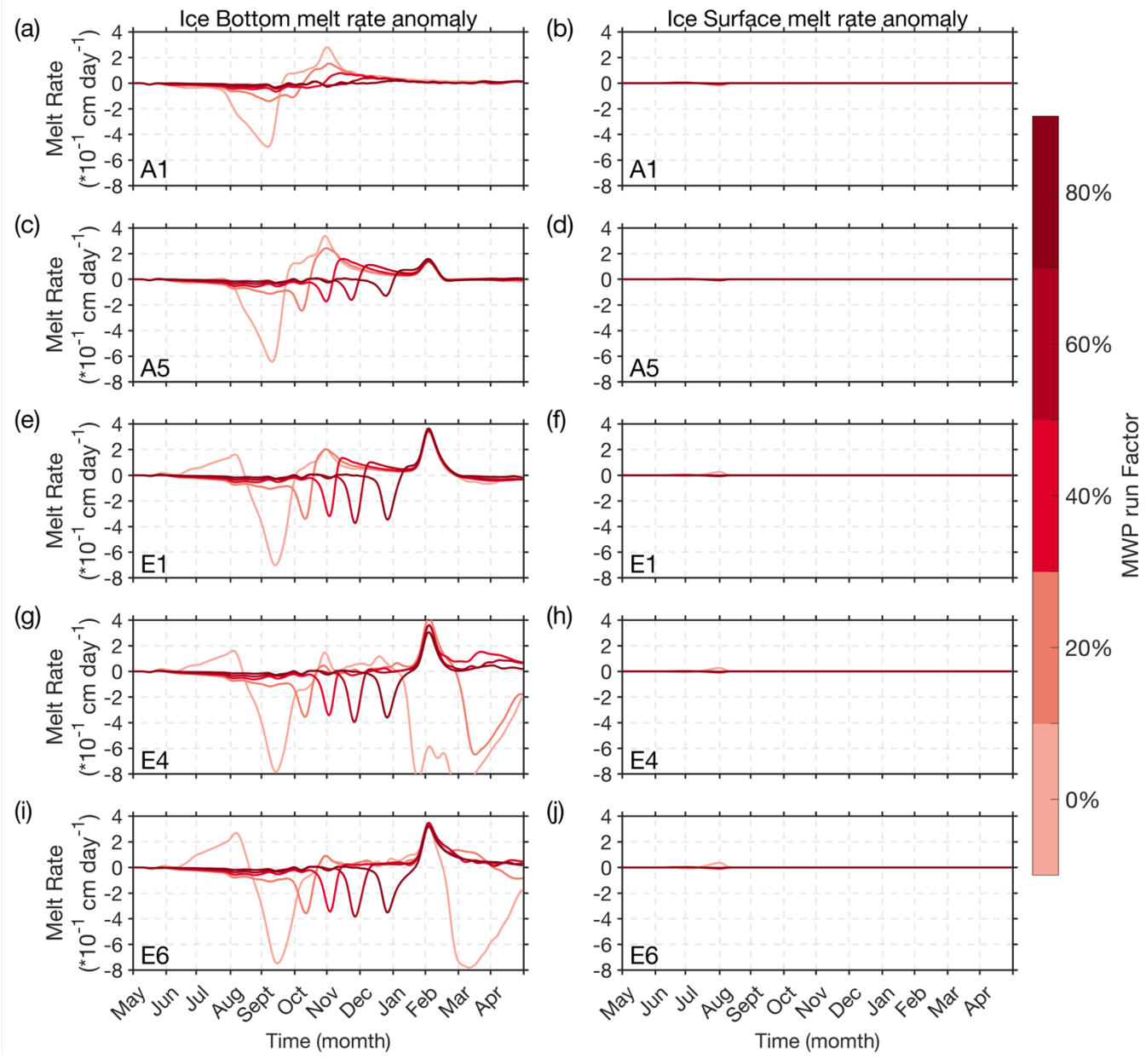

Figure 12: Time series of the (left) ice bottom melt rate anomaly and (right) ice surface melt rate anomaly of the MWP runs for stations A1, A5, E1, E4, and E6. The colour of each line represents the MWP run factor.

https://doi.org/10.5194/egusphere-2023-477
Preprint. Discussion started: 21 March 2023

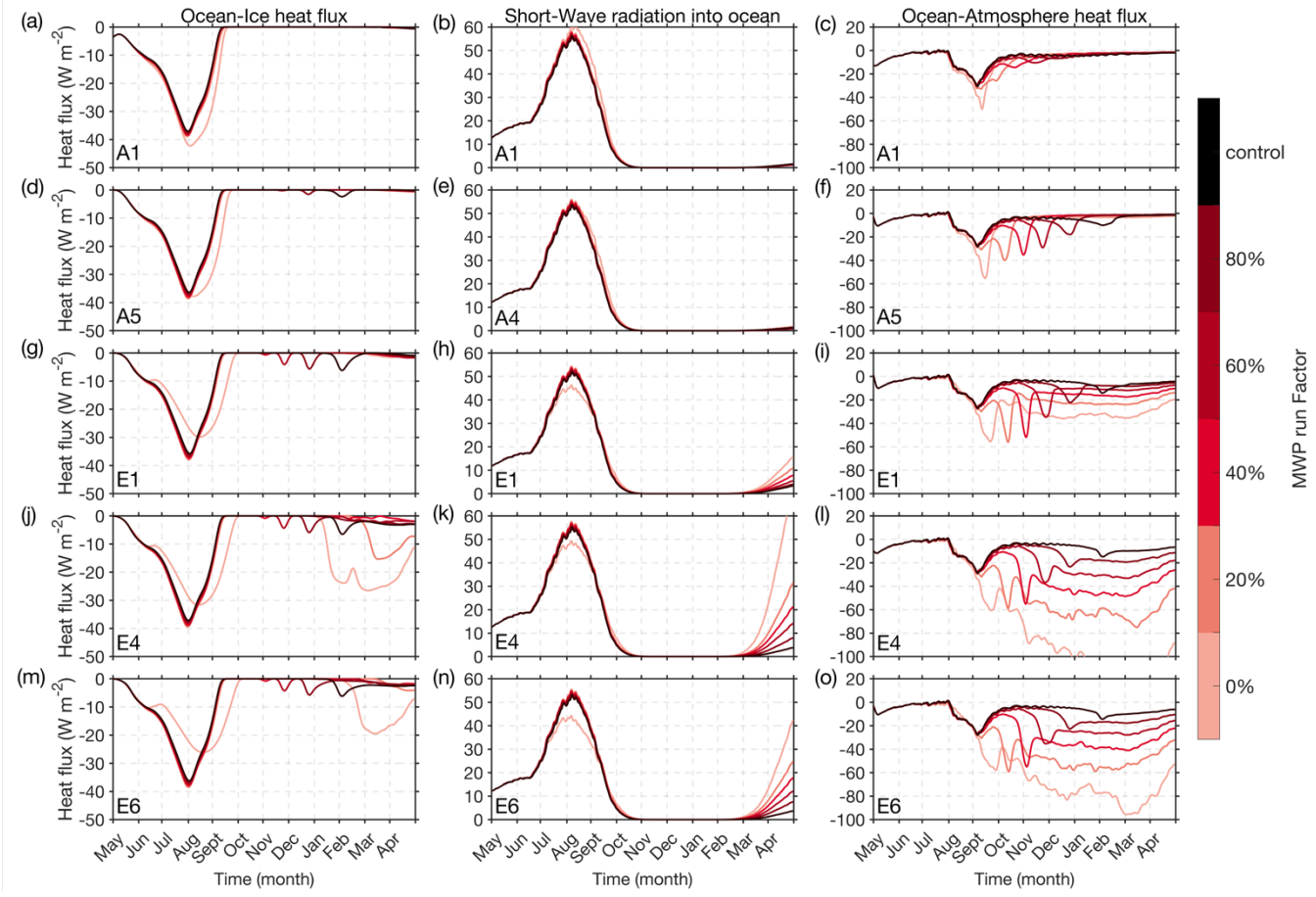

290 **Figure 13: Time series of the (left) ocean to ice heat flux (F_b), (middle) shortwave radiation into the ocean (F_{sw}), and (right) ocean to atmosphere heat flux (F_{ao}) for stations A1, A5, E1, E4 and E6, with negative values representing the loss of heat from the ocean.**

In the MWP-0% runs, the NSTM promotes ice bottom melting in two ways. The first way, which is dominant in well-stratified areas, is by directly heating the ice bottom by upwards mixing in summer, resulting in faster melting, and the other way, which is dominant in areas with weaker stratification, is by prolonging the ice-melting season. For example, at station
295 A1, where the stratification is strong, the ice bottom melting rate (Fig. 12a) and ocean ice heat flux (Fig. 13a) are greater in the MWP-0% run than the control run throughout the whole summer, while at station E6, where stratification is weak, the ice bottom melting rate (Fig. 12i) and ocean ice heat flux (Fig. 13m) are not greater in the MWP-0% run than the control run until late summer. The reason is that in the strongly stratified stations, even when all meltwater is removed, the stratification is still strong, and the heat stored in the NSTM is mixed only upwards and used for ice melting, whereas at a weakly stratified station,
300 the heat is not only mixed upwards but also mixed downwards. The heat transferred downwards to the lower mixed layer mixes upwards at the onset of the freezing season, which delays the freeze-up and prolongs the ice-melting season. This mechanism explains why meltwater has less impact on sea ice melting in areas with weak stratification. After removal of meltwater, the amount of heat stored in the NSTM that is used for ice melting is larger in the strongly stratified region than in the weakly

https://doi.org/10.5194/egusphere-2023-477
Preprint. Discussion started: 21 March 2023

stratified region. In the MWP-0% run, at stations E4-6, sea ice melt increases by approximately 7–13% during the melting season compared to the control run, while at stations A1–5, sea ice melt increases by approximately 19% (Fig. 11a).

b) Freezing season

Figure 10c shows the effective sea ice thickness changes from the minimum value in summer to the end of the freezing season in the sensitivity experiments for all stations. The winter sea ice formation at the strongly stratified stations A1–5 and E1-2 is inversely proportional to the amount of meltwater released in previous melting season. In the MWP-0% run, an average increase in sea ice thickness of 22.5 cm (approximately 12.8%) was simulated at these stations compared to the control run. Sea ice formation at stations E3 and E4 is less sensitive to meltwater release changes than that at other stations. In contrast, at the weakly stratified stations E5 and E6, sea ice formation in the MWP-0% runs decreases by an average of 92.1 cm (57.4%) compared to the control run (Figs. 10b and 11b).

At some stations with strong haloclines, e.g., stations A1-3, even with all the meltwater removed, the halocline is still strong, which can effectively prevent the mixed layer from deepening in winter, as discussed in section 3.2.1. Moreover, the reduction in summer meltwater results in a colder mixed layer, a larger area of open water, and a weaker or even absent NSTM, causing the water temperature to drop more quickly to the freezing point during winter and leading to increased ice formation. However, at some stations with a weak halocline, e.g., stations E5 and E6, the complete removal of meltwater allows a deep mixed layer to be formed, and the Atlantic warm water can reach the surface, which effectively prevents the formation of sea ice. In addition, in March, the mixed layer can reach the depth of the warm Atlantic water, and a large amount of heat from the warm Atlantic water mixes upwards and heats the sea ice, leading to early melting of the sea ice (such as Fig. 9i), which allows large areas of open water to exist during the winter (such as Fig. 9j), thus enabling the sea surface to absorb more solar radiation in winter (Fig. 13k and n), allowing heat from the warm Atlantic water to enter the atmosphere, and the ocean-atmosphere heat flux can reach 100 W/m2 in March at station E6 (Fig. 13p).

The results indicate that the effect of the reduced meltwater release on ice formation gradually transitions from promoting to prohibiting ice growth as the halocline weakens. This means that meltwater has negative feedback on ice formation in areas with strong stratification and positive feedback in areas with weak stratification (Fig. 11b).

c) Annual net sea ice changes

The annual net changes in the effective ice thickness for the control run and MWP runs at all stations are shown in Fig. 10e. In strongly stratified regions (such as stations A1-A5 and E1-E2), the annual net sea ice change is insensitive to meltwater release (Fig. 10e) because the reduction in meltwater not only leads to more sea ice melting in summer but also leads to an increase in ice formation during winter (Fig. 10c), which offsets the extra ice melting in summer. In weakly stratified regions (stations E3-E6), the annual net sea ice change is more sensitive to meltwater release (Fig. 10e) because the reduction in meltwater induces a deeper mixed layer and enhances the ocean ice heat flux, resulting in insufficient sea ice formation in winter, which cannot compensate for the extra summer ice melting.

In summary, the above results indicate that meltwater always has negative feedback on ice melting, but it has negative feedback on ice formation in strongly stratified areas and positive feedback in weakly stratified areas. The meltwater obstructs

https://doi.org/10.5194/egusphere-2023-477
Preprint. Discussion started: 21 March 2023

upwards heat transfer from the NSTM to the ice cover, which is the main reason for the negative feedback of meltwater on sea ice melting during summer. In addition, the meltwater significantly inhibits ice melt at stations E5 and E6 by hindering the upwards heat flux from warm AW in spring.

4 Conclusions

In this study, the responses of upper ocean stratification and sea ice growth/melt in the Arctic Ocean to meltwater release are investigated using a one-dimensional coupled sea ice-ocean model. We perform two types of experiments to achieve the goals: a control run and five meltwater perturbation experiments with 0%, 20%, 40%, 60%, and 80% meltwater release into the ocean.

Compared to the observations, the one-dimensional coupled sea ice-ocean model reproduces the observed temperature and salinity structure of the Arctic Ocean reasonably well, capturing important features such as the fresh surface layer, the near-surface temperature maximum (NSTM), and the seasonal variation in MLD. In the control runs, the results suggest that ice growth depends on ocean stratification because weaker ocean stratification leads to higher ocean ice heat flux during winter. In the meltwater perturbation experiments, as expected, decreasing meltwater increases the salinity of the surface and weakens stratification, flattening the upper halocline and changing the vertical heat flux from the depth to the surface. These changes subsequently affect the melting or formation of sea ice. Our results suggest that a decrease in meltwater release has the following effects on sea ice:

1. During the melting season, meltwater has an inhibitory effect on sea ice melt by preventing the NSTM from mixing upwards. The minimum summer effective sea ice thickness values in the control runs are 7-19% greater than those of the MWP-0% runs, suggesting that the presence of meltwater exerts negative feedback on the process of sea ice melt that is more significant in stations with strong stratification (Fig. 11a).
2. During the freezing season, the effect of meltwater released in the previous melting season on sea ice growth varies with ocean stratification. In regions with weaker stratification, such as the Nansen Basin, meltwater plays a more important role in maintaining sea ice and ocean stratification than in areas with stronger stratification, such as the Canadian Basin. The model results show that at strongly stratified stations, the net increase in winter effective sea ice thickness in the control run is 12-14% smaller than that in the MWP-0% run. Conversely, at weakly stratified stations, the net increase in effective sea ice thickness in the control run is 42-73% larger than that in the MWP-0% run. These results indicate that the feedback effect of meltwater on sea ice growth is affected by the strength of stratification, resulting in negative feedback from meltwater on winter sea ice growth in areas of strong stratification and positive feedback in areas of weak stratification (Fig. 11b).

https://doi.org/10.5194/egusphere-2023-477
Preprint. Discussion started: 21 March 2023

5 Discussion

A key finding of this study is that the impact of meltwater on feedback mechanisms varies based on the strength of ocean stratification. This suggests that the ice-covered Arctic Ocean can be divided into two regimes based on ocean stratification: some areas with strong stratification that are less sensitive to meltwater, where the meltwater only prevents the NSTM from melting ice, and other small areas with weak stratification that are more sensitive to melt water, where the meltwater not only prevents NSTM from melting ice in the summer but also prevents warm AW from mixing upwards in early spring. The border between these two regimes depends on ocean stratification. Stations E4 and E5 are clear examples. The initial CHL at station E5 is quite weak (Fig. 2f), and the AW is mixed sufficiently upwards in the spring after removing the meltwater. Station E4, close to station E5, has a relatively stronger initial CHL than station E5 (Fig. 2f), and the AW cannot reach the upper ocean and ice even when the meltwater is removed.

Wang et al. (2019) noted that although sea ice decline does not change the total Arctic liquid freshwater content (FWC), the increase in the liquid FWC in the Amerasian basin is nearly compensated by the reduction in the Eurasian basin, which results in significant changes in the spatial distribution of the liquid FWC. This raises the question of how the exchange of meltwater between these two regimes in the Arctic Ocean will affect the ocean and sea ice. From our experimental results, it appears that if meltwater or liquid FWC from other sources is continuously lost outwards from an area during the melting season, then the sea ice in that area will melt more rapidly; if this area occurs where the meltwater will have a significant impact (e.g., E5, E6), then there is a high probability that the AW will mix sufficiently upwards during the freezing season and reach the ice cover, which can cause substantial sea ice melting and prolong the melting season. The warm AW plays an important role in reducing the sea ice cover in the Arctic Ocean through upwards heat loss (Polyakov et al., 2010) because the heat contained within the AW layer is sufficient to melt all sea ice in the Arctic within a few years (Turner, 2010). Climate model projections suggest that freshwater input from enhanced river runoff and positive precipitation minus evaporation (P-E) will increase by ~30% by 2050 (Peterson et al., 2002; Bintanja and Selten, 2014; Haine et al., 2015). Increased freshwater input, like more meltwater entering the ocean, can strengthen the cold halocline by increasing the magnitude of the salinity gradient, which will also inevitably create feedback on sea ice melt, especially in some important areas such as stations E5 and E6 in this study.

A limitation of the 1-D model is that it cannot directly represent the effect of lateral variations in the upper ocean in combination with ocean/ice advection. Advection is of great importance when performing long-term simulations and should be addressed, for example, by introducing some type of restoration of the profiles towards the observed values (Polyakov et al., 2010). For shorter simulations and relatively horizontally constant TS properties, it can be assumed that advection will have a smaller effect (Linders and Björk, 2013). The non-advective approach can be justified if the ice does not drift too far relative to the initial water column over the simulation period. This can be valid for only a limited period of time. Thus, our computations are conducted only over a single freezing-melting season. In this study, we focus on the effects of meltwater on

https://doi.org/10.5194/egusphere-2023-477
Preprint. Discussion started: 21 March 2023

vertical processes in the ocean and do not consider the effects of advection, and the simulations are short (1 year). Therefore, the results of the 1-D mode used in this study can be justified.

In our simulation, the initial thickness of the sea ice is set to 2.5 m, and the study does not discuss the impact of the initial sea ice thickness variability. In fact, the albedo of sea ice varies with its thickness, so under the same atmospheric forcing, sea ice with different initial thicknesses will exhibit different seasonal variations (Linders and Björk, 2013). Therefore, it can be inferred that the feedback effects of melting water may also differ for sea ice with different initial thicknesses. For instance, thicker ice has a higher albedo and produces less meltwater, resulting in lower temperatures in the NSTM, which could lead to a decrease in the feedback effect of meltwater. However, this difference may be relatively small and will not affect our main conclusion.

This study provides valuable insights into the intricate relationships between ocean stratification, meltwater, and sea ice growth and their implications for predicting future changes in the Arctic region. Understanding these complex interactions is essential for developing accurate climate models and assessing the potential impacts of climate change on the Arctic ecosystem. The study in this paper addresses only the effects of meltwater in the vertical direction, and future work could focus on the effects of meltwater transport processes during the melting season in conjunction with Arctic Ocean circulation. To address this issue, more detailed modelling, including advection processes, is needed.

Data availability

The Ice-Tethered Profiler data are collected and made available by the Ice-Tethered Profiler Program (Krishfield et al., 2008; Toole et al., 2010) based at the Woods Hole Oceanographic Institution (https://www2.whoi.edu/site/itp/). NCEP/DOE Reanalysis II data provided by the NOAA PSL, Boulder, Colorado, USA (https://psl.noaa.gov). The numerical model configuration, parameters, forcing fields and the simulation results used in this paper are stored at https://zenodo.org/record/7727849#.ZA7nuOtBxTY.

Author contributions

HH designed and conducted the experiments, analyzed the experimental data, and drafted the initial version of the manuscript. XZ conceived the idea for the study, participated in writing the manuscript, and made several significant revisions to it. KW contributed to the analysis of experimental data. All authors have reviewed and approved the final version of the manuscript.

Competing interests

Neither of the authors has any competing interests.

https://doi.org/10.5194/egusphere-2023-477
Preprint. Discussion started: 21 March 2023

Acknowledgements

This work was funded by the National Key Research and Development Program of China (Grant 2017YFA0604602), the National Natural Science Foundation of China (Grant 42276254), and the Postgraduate Research & Practice Innovation Program of Jiangsu Province (Grant KYCX19_0384).

References

Bintanja, R. and Selten, F. M.: Future increases in Arctic precipitation linked to local evaporation and sea-ice retreat, Nature, 509, 479–482, https://doi.org/10.1038/nature13259, 2014.

Bitz, C. M. and Lipscomb, W. H.: An energy-conserving thermodynamic model of sea ice, J. Geophys. Res. Oceans, 104, 15669–15677, https://doi.org/10.1029/1999JC900100, 1999.

Bitz, C. M., Battisti, D. S., Moritz, R. E., and Beesley, J. A.: Low-frequency variability in the arctic atmosphere, sea ice, and upper-ocean climate system, J. Climate, 9, 394–408, https://doi.org/10.1175/1520-0442(1996)009<0394:lfvita>2.0.co;2, 1996.

Björk, G.: Return of the cold halocline layer to the Amundsen basin of the Arctic ocean: implications for the sea ice mass balance, Geophys. Res. Lett., 29, 1513, https://doi.org/10.1175/JPO-D-15-0174.1, 2002a.

Björk, G.: Dependence of the Arctic ocean ice thickness distribution on the poleward energy flux in the atmosphere, J. Geophys. Res., 107, 3173, https://doi.org/10.1029/2000jc000723, 2002b.

Davis, P. E. D., Lique, C., Johnson, H. L., and Guthrie, J. D.: Competing effects of elevated vertical mixing and increased freshwater input on the stratification and sea ice cover in a changing Arctic ocean, J. Phys. Oceanogr., 46, 1531–1553, https://doi.org/10.1175/jpo-d-15-0174.1, 2016.

Fer, I.: Weak vertical diffusion allows maintenance of cold halocline in the Central Arctic, Atmospheric and Oceanic Science Letters, 2, 148–152, https://doi.org/10.1080/16742834.2009.11446789, 2009.

Haine, T. W. N., Curry, B., Gerdes, R., Hansen, E., Karcher, M., Lee, C., Rudels, B., Spreen, G., de Steur, L., Stewart, K. D., and Woodgate, R.: Arctic freshwater export: status, mechanisms, and prospects, Global Planet. Change, 125, 13–35, https://doi.org/10.1016/j.gloplacha.2014.11.013, 2015.

Hordoir, R., Skagseth, Ø., Ingvaldsen, R. B., Sandø, A. B., Löptien, U., Dietze, H., Gierisch, A. M. U., Assmann, K. M., Lundesgaard, Ø., and Lind, S.: Changes in Arctic stratification and mixed layer depth cycle: a modeling analysis, J. Geophys. Res. Oceans, 127, e2021JC017270, https://doi.org/10.1029/2021jc017270, 2022.

Jackett, D. R. and McDougall, T. J.: Minimal adjustment of hydrographic profiles to achieve static stability, J. Atmos. Ocean. Tech., 12, 381–389, https://doi.org/10.1175/1520-0426(1995)012<0381:maohpt>2.0.co;2, 1995.

Jackson, J. M., Carmack, E. C., McLaughlin, F. A., Allen, S. E., and Ingram, R. G.: Identification, characterization, and change of the near-surface temperature maximum in the Canada Basin, 1993–2008, J. Geophys. Res., 115, C05021, https://doi.org/10.1029/2009jc005265, 2010.

https://doi.org/10.5194/egusphere-2023-477
Preprint. Discussion started: 21 March 2023

Killworth, P. D. and Smith, J. M.: A one-and-a-half dimensional model for the Arctic halocline, Deep Sea Research Part A. Oceanographic Research Papers, 31, 271–293, https://doi.org/10.1016/0198-0149(84)90105-5, 1984.

Krishfield, R., Toole, J., Proshutinsky, A., and Timmermans, M. L.: Automated ice-tethered profilers for seawater observations under pack ice in all seasons, J. Atmos. Ocean. Tech., 25, 2091–2105, https://doi.org/10.1175/2008jtecho587.1, 2008.

Large, W. G., McWilliams, J. C., and Doney, S. C.: Oceanic vertical mixing: a review and a model with a nonlocal boundary layer parameterization, Rev. Geophys., 32, 363, https://doi.org/10.1029/94rg01872, 1994.

Linders, J. and Björk, G.: The melt-freeze cycle of the Arctic ocean ice cover and its dependence on ocean stratification, J. Geophys. Res. Oceans, 118, 5963–5976, https://doi.org/10.1002/jgrc.20409, 2013.

Losch, M., Menemenlis, D., Campin, J.-M., Heimbach, P., and Hill, C.: On the formulation of sea-ice models. Part 1: effects of different solver implementations and parameterizations, Ocean Model., 33, 129–144, https://doi.org/10.1016/j.ocemod.2009.12.008, 2010.

Marshall, J., Hill, C., Perelman, L., and Adcroft, A.: Hydrostatic, quasi-hydrostatic, and nonhydrostatic ocean modeling, J. Geophys. Res. Oceans, 102, 5733–5752, https://doi.org/10.1029/96jc02776, 1997.

Martinson, D. G. and Steele, M.: Future of the Arctic sea ice cover: implications of an Antarctic analog, Geophys. Res. Lett., 28, 307–310, https://doi.org/10.1029/2000gl011549, 2001.

McClelland, J. W., Holmes, R. M., Dunton, K. H., and Macdonald, R. W.: The Arctic ocean estuary, Estuar. Coast., 35, 353–368, https://doi.org/10.1007/s12237-010-9357-3, 2012.

Nummelin, A., Li, C., and Smedsrud, L. H.: Response of Arctic ocean stratification to changing river runoff in a column model, J. Geophys. Res. Oceans, 120, 2655–2675, https://doi.org/10.1002/2014jc010571, 2015.

Nummelin, A., Ilicak, M., Li, C., and Smedsrud, L. H.: Consequences of future increased Arctic runoff on Arctic ocean stratification, circulation, and sea ice cover, J. Geophys. Res. Oceans, 121, 617–637, https://doi.org/10.1002/2015jc011156, 2016.

Pemberton, P. and Nilsson, J.: The response of the central Arctic ocean stratification to freshwater perturbations, J. Geophys. Res. Oceans, 121, 792–817, https://doi.org/10.1002/2015jc011003, 2016.

Peralta-Ferriz, C. and Woodgate, R. A.: Seasonal and interannual variability of pan-Arctic surface mixed layer properties from 1979 to 2012 from hydrographic data, and the dominance of stratification for multiyear mixed layer depth shoaling, Prog. Oceanogr., 134, 19–53, https://doi.org/10.1016/j.pocean.2014.12.005, 2015.

Perovich, D. K. and Maykut, G. A.: The treatment of shortwave radiation and open water in large-scale models of sea-ice decay, Ann. Glaciol., 14, 242–246, https://doi.org/10.3189/s0260305500008673, 1990.

Peterson, B. J., Holmes, R. M., McClelland, J. W., Vörösmarty, C. J., Lammers, R. B., Shiklomanov, A. I., Shiklomanov, I. A., and Rahmstorf, S.: Increasing river discharge to the Arctic ocean, Science, 298, 2171–2173, https://doi.org/10.1126/science.1077445, 2002.

Polyakov, I. V., Timokhov, L. A., Alexeev, V. A., Bacon, S., Dmitrenko, I. A., Fortier, L., Frolov, I. E., Gascard, J.-C., Hansen, E., Ivanov, V. V., Laxon, S., Mauritzen, C., Perovich, D., Shimada, K., Simmons, H. L., Sokolov, V. T., Steele, M.,

https://doi.org/10.5194/egusphere-2023-477
Preprint. Discussion started: 21 March 2023

and Toole, J.: Arctic ocean warming contributes to reduced polar ice cap, J. Phys. Oceanogr., 40, 2743–2756, https://doi.org/10.1175/2010jpo4339.1, 2010.

Price, J. F., Weller, R. A., and Pinkel, R.: Diurnal cycling: observations and models of the upper ocean response to diurnal heating, cooling, and wind mixing, J. Geophys. Res., 91, 8411, https://doi.org/10.1029/jc091ic07p08411, 1986.

Rawlins, M. A., Steele, M., Holland, M. M., Adam, J. C., Cherry, J. E., Francis, J. A., Groisman, P. Y., Hinzman, L. D., Huntington, T. G., Kane, D. L., Kimball, J. S., Kwok, R., Lammers, R. B., Lee, C. M., Lettenmaier, D. P., McDonald, K. C., Podest, E., Pundsack, J. W., Rudels, B., Serreze, M. C., Shiklomanov, A., Skagseth, Ø., Troy, T. J., Vörösmarty, C. J., Wensnahan, M., Wood, E. F., Woodgate, R., Yang, D., Zhang, K., and Zhang, T.: Analysis of the Arctic system for freshwater cycle intensification: observations and expectations, J. Climate, 23, 5715–5737, https://doi.org/10.1175/2010jcli3421.1, 2010.

Rudels, B.: Arctic ocean circulation, processes and water masses: a description of observations and ideas with focus on the period prior to the International Polar Year 2007–2009, Prog. Oceanogr., 132, 22–67, https://doi.org/10.1016/j.pocean.2013.11.006, 2015.

Rudels, B., Anderson, L. G., and Jones, E. P.: Formation and evolution of the surface mixed layer and halocline of the Arctic ocean, J. Geophys. Res. Oceans, 101, 8807–8821, https://doi.org/10.1029/96jc00143, 1996.

Rudels, B., Björk, G., Nilsson, J., Winsor, P., Lake, I., and Nohr, C.: The interaction between waters from the Arctic ocean and the Nordic seas north of fram strait and along the East Greenland current: results from the Arctic ocean-02 Oden expedition, J. Marine Syst., 55, 1–30, https://doi.org/10.1016/j.jmarsys.2004.06.008, 2005.

Shaw, W. J., Stanton, T. P., McPhee, M. G., Morison, J. H., and Martinson, D. G.: Role of the upper ocean in the energy budget of Arctic sea ice during SHEBA, J. Geophys. Res., 114, C06012, https://doi.org/10.1029/2008jc004991, 2009.

Shimada, K., Carmack, E. C., Hatakeyama, K., and Takizawa, T.: Varieties of shallow temperature maximum waters in the Western Canadian basin of the Arctic ocean, Geophys. Res. Lett., 28, 3441–3444, https://doi.org/10.1029/2001gl013168, 2001.

Sirevaag, A., de la Rosa, S., Fer, I., Nicolaus, M., Tjernström, M., and McPhee, M. G.: Mixing, heat fluxes and heat content evolution of the Arctic Ocean mixed layer, mixed layer/in situ observations/deep seas: arctic ocean/turbulence and mixing, https://doi.org/10.5194/osd-8-247-2011, 2011.

Steele, M.: Salinity trends on the Siberian shelves, Geophys. Res. Lett., 31, L24308, https://doi.org/10.1029/2004gl021302, 2004.

Steele, M. and Boyd, T.: Retreat of the cold halocline layer in the Arctic ocean, J. Geophys. Res. Oceans, 103, 10419–10435, https://doi.org/10.1029/98jc00580, 1998.

Steele, M., Zhang, J., and Ermold, W.: Mechanisms of summertime upper Arctic ocean warming and the effect on sea ice melt, J. Geophys. Res., 115, C11004, https://doi.org/10.1029/2009jc005849, 2010.

https://doi.org/10.5194/egusphere-2023-477
Preprint. Discussion started: 21 March 2023

Toole, J. M., Timmermans, M. L., Perovich, D. K., Krishfield, R. A., Proshutinsky, A., and Richter-Menge, J. A.: Influences of the ocean surface mixed layer and thermohaline stratification on Arctic sea ice in the central Canada basin, J. Geophys. Res. Oceans, 115, 2009JC005660, https://doi.org/10.1029/2009jc005660, 2010.

Turner, J. S.: The melting of ice in the Arctic ocean: the influence of double-diffusive transport of heat from below, J. Phys. Oceanogr., 40, 249–256, https://doi.org/10.1175/2009jpo4279.1, 2010.

Wang, Q., Wekerle, C., Danilov, S., Sidorenko, D., Koldunov, N., Sein, D., Rabe, B., and Jung, T.: Recent sea ice decline did not significantly increase the total liquid freshwater content of the Arctic ocean, J. Climate, 32, 15–32, https://doi.org/10.1175/jcli-d-18-0237.1, 2019.

Winton, M.: A reformulated three-layer sea ice model, J. Atmos. Ocean. Tech., 17, 525–531, https://doi.org/10.1175/1520-0426(2000)017<0525:artlsi>2.0.co;2, 2000.